PHYSICAL REVIEW B **83**, 081408(R) (2011)

Plasmon polariton and $\langle n \rangle = 0$ non-Bragg gaps in superlattices with metamaterials

C. A. A. de Carvalho,[1] S. B. Cavalcanti,[2] E. Reyes-Gómez,[3] and L. E. Oliveira[4]

[1]*Instituto de Física, UFRJ, Rio de Janeiro-RJ, 21945-972, Brazil*
[2]*Instituto de Física, UFAL, Cidade Universitária, 57072-970, Maceió-AL, Brazil*
[3]*Instituto de Física, Universidad de Antioquia, AA 1226, Medellín, Colombia*
[4]*Instituto de Física, UNICAMP, Campinas-SP, 13083-859, Brazil*

(Received 29 November 2010; revised manuscript received 30 December 2010; published 16 February 2011)

We consider one-dimensional photonic superlattices made up of alternate layers of a right-handed nondispersive material and a metamaterial with Drude-type dielectric permittivity and magnetic permeability. By thoroughly investigating the dispersion relation for the propagation of obliquely incident optical fields obtained from Maxwell's equations and the transfer-matrix technique, we demonstrate that, in the long-wavelength limit, the dispersion is the same that one would obtain by considering a homogeneous effective medium with Drude-type responses at shifted electric and magnetic plasmon frequencies. Moreover, we show that the plasmon polariton and $\langle n \rangle = 0$ non-Bragg gaps correspond to regions of the low-energy spectrum where the effective medium is absorptive, exhibiting an imaginary effective refraction index.

DOI: 10.1103/PhysRevB.83.081408 PACS number(s): 78.20.Bh, 41.20.Jb, 42.70.Gi, 42.70.Qs

In the last two decades or so, the realization of artificially complex materials has allowed for the possibility of tailoring the electromagnetic dispersions and mode structures to suit almost any need. The advent of metamaterials[1–9] has opened a new era for photonic devices made possible by conveniently shaping and manipulating light. It has also given considerable thrust to the recent area of plasmonics that deals with the generation, propagation, and detection of plasmon polaritons (PPs), which are collective electronic and magnetic excitations generated by a resonant electromagnetic field. A typical example of a metamaterial is provided by a dispersive[10] left-handed material (LHM) that exhibits negative refraction. In a LHM, the light phase velocity points to the opposite direction relative to the flow of energy, in contrast with a right-handed material (RHM). LHMs have exhibited exciting new possibilities in light manipulation that were considered as science fiction in the last century, such as super lenses[11] and cloaking.[12,13] Such LHMs may be designed to exhibit optical magnetism in the sense that the magnetic component of the optical field plays an active role in its interaction with light, i.e., nanomaterials involving magnetically active LHMs should reveal many unexpected features to be utilized in nanoelectronics as well as in nanomagnetonics in the quest for nanodevices. Of course, within the context of nanophotonics, plasmonics (based on PP propagation) is a very promising area of research.

Recent studies on the propagation of light obliquely incident in one-dimensional (1D) stacks of a periodic (or quasiperiodic) arrangement characterized by the repetition of a unit double-layer cell composed of an usual RHM (A layer) and a dispersive LHM (B layer), henceforth referred to as metastacks, have revealed unusual features. For example, the null-average refractive index non-Bragg gap[14,15] and longitudinal PP modes of both magnetic (in a transversal electric (TE) configuration) and electric (in a transversal magnetic (TM) configuration) nature[16,17] have been reported in such metastacks. Disordered metastacks have also exhibited essentially the same features.[18]

In this paper, we study the oblique incidence of light on a model 1D superlattice composed of layers A of a right-handed nondispersive material, and layers B of a doubly negative material. Layers A (width a) and B (width b) are distributed periodically so that $d = a + b$ is the period of the superlattice nanostructure. In the B layers, the electric and magnetic responses are dispersive and may assume negative values. If one neglects losses, they may be described by Drude-type responses given by[10]

$$\varepsilon_B(\omega) = \varepsilon_0 - \frac{\omega_e^2}{\omega^2}, \quad \mu_B(\omega) = \mu_0 - \frac{\omega_m^2}{\omega^2}, \tag{1}$$

where $\varepsilon_B(\omega)$ and $\mu_B(\omega)$ are the dielectric permittivity and magnetic permeability in slab B, respectively. One may choose $\varepsilon_0 = 1.21$ and $\mu_0 = 1.0$, and the electric (magnetic) plasmon modes are at $\omega = \bar{\omega}_e = \frac{\omega_e}{\sqrt{\epsilon_0}}$ and $\omega = \bar{\omega}_m = \frac{\omega_m}{\sqrt{\mu_0}}$, which correspond to the solutions of $\epsilon_B(\omega) = 0$ and $\mu_B(\omega) = 0$, respectively. The index of refraction of layer B is given by

$$n_B^2 = \mu_B \varepsilon_B = \mu_0 \varepsilon_0 \left(1 - \frac{\bar{\omega}_m^2}{\omega^2}\right)\left(1 - \frac{\bar{\omega}_e^2}{\omega^2}\right), \tag{2}$$

so that $\bar{\omega}_m$ and $\bar{\omega}_e$ are the roots of $n_B(\omega) = 0$. Thus, we have

$$\begin{aligned} \omega < \min(\bar{\omega}_m, \bar{\omega}_e) &\Rightarrow n_B^2 > 0, \\ \min(\bar{\omega}_m, \bar{\omega}_e) < \omega < \max(\bar{\omega}_m, \bar{\omega}_e) &\Rightarrow n_B^2 < 0, \\ \omega > \max(\bar{\omega}_m, \bar{\omega}_e) &\Rightarrow n_B^2 > 0. \end{aligned} \tag{3}$$

We shall analyze the TE dispersion relation obtained from the transfer-matrix method,[15–20] in the case $n_B^2 - n_A^2 \sin^2\theta > 0$, i.e.,

$$\begin{aligned} \cos(kd) = &\cos(Q_A a)\cos(Q_B b) \\ &- \frac{1}{2}\left(\frac{F_A}{F_B} + \frac{F_B}{F_A}\right)\sin(Q_A a)\sin(Q_B b). \end{aligned} \tag{4}$$

In this formula, k is the Bloch wave vector along the z direction, which is the axis of the photonic crystal; fields in consecutive unit cells are related by the Bloch condition, i.e., by the phase factor e^{ikd}. Q_A and Q_B are defined as

$$Q_A = \frac{\omega}{c} n_A |\cos\theta| = \frac{\omega}{c} n_A |\cos\theta_A| \tag{5}$$

and

$$Q_B = \frac{\omega}{c}\sqrt{n_B^2 - n_A^2 \sin^2\theta} = \frac{\omega}{c}|n_B||\cos\theta_B|, \tag{6}$$

where $F_A = (Q_A/\mu_A)$, $F_B = (Q_B/\mu_B)$, and, in the last equality, we have made use of Snell's law $n_A \sin\theta = n_B \sin\theta_B$.

First, we will assume that $Q_A a \ll 1$, $Q_B b \ll 1$, and look at the long-wavelength limit $kd \ll 1$. Let us begin by investigating the case $k = 0$, i.e., the center of the Brillouin zone. Expanding the right-hand side (RHS) of Eq. (4), we derive

$$(a\mu_A + b\mu_B)\left(\frac{aQ_A^2}{\mu_A} + \frac{bQ_B^2}{\mu_B}\right) \simeq 0 \tag{7}$$

with roots given by

$$a\mu_A + b\mu_B \simeq 0, \tag{8}$$

$$\frac{aQ_A^2}{\mu_A} + \frac{bQ_B^2}{\mu_B} \simeq 0. \tag{9}$$

Equation (8) may be interpreted as corresponding to a null-average magnetic permeability of the superlattice nanostructure, i.e.,

$$\langle\mu\rangle = \frac{a\mu_A + b\mu_B(\omega)}{d} \simeq 0, \tag{10}$$

and, from the previous equation, one obtains a mode at $\omega = \omega_\mu$ such that

$$\mu_B(\omega_\mu) \simeq -\frac{a}{b}\mu_A. \tag{11}$$

Using the Drude-type expression for the μ_B magnetic permeability, Eq. (11) yields

$$\omega_\mu^2 = \left(\frac{b\mu_0}{a\mu_A + b\mu_0}\right)\bar{\omega}_m^2. \tag{12}$$

From Eq. (9), and using the Drude-type expression for ϵ_B, we obtain two additional roots

$$\omega_\pm^2 = \frac{\left[l_\theta\varepsilon_A\omega_m^2 + b\mu_0\omega_e^2 + b\varepsilon_0\omega_m^2(1-\varepsilon_A)\right] \pm \sqrt{\left[l_\theta\varepsilon_A\omega_m^2 - b\mu_0\omega_e^2 + b\varepsilon_0\omega_m^2(1-\varepsilon_A)\right]^2 + 4b^2\mu_A\varepsilon_A\omega_m^2\omega_e^2\sin^2\theta}}{2L_\theta}, \tag{13}$$

with $l_\theta \equiv b\,\varepsilon_0 + a\cos^2\theta$ and $L_\theta \equiv \mu_0\varepsilon_A l_\theta + b\mu_0\varepsilon_0(1-\varepsilon_A) - b\mu_A\varepsilon_A\sin^2\theta$. Here we note that Eqs. (12) and (13) yield three roots and, as we will see in the sequel, they define both the $\langle n\rangle = 0$ and the plasmon-polariton gaps that appear at $k = 0$ and $\theta \neq 0$.

First, however, let us look at normal incidence $\theta = 0$. In this case, the dispersion Eq. (7) yields

$$(\mu_A a + \mu_B b)(\varepsilon_A a + \varepsilon_B b) \simeq 0, \tag{14}$$

which corresponds to $\langle\mu\rangle\langle\varepsilon\rangle \simeq 0$. By using the Drude expressions (14) (at $k = 0$ and $\theta = 0$), one finds only *two* roots:

$$\omega_\mu^2 = \left(\frac{b\mu_0}{a\mu_A + b\mu_0}\right)\bar{\omega}_m^2, \tag{15}$$

which comes from the vanishing of the first term in parentheses, and

$$\omega_\varepsilon^2 = \left(\frac{b\varepsilon_0}{a\varepsilon_A + b\varepsilon_0}\right)\bar{\omega}_e^2, \tag{16}$$

which comes from the vanishing of the second term in parentheses. Note that $l_0 = a\varepsilon_A + b\varepsilon_0$. By expanding Eq. (4) for $kd \gg 1$ to the lowest order, one finds

$$k^2 \simeq \frac{\omega^2}{c^2}\left[\frac{a^2\varepsilon_A\mu_A + b^2\varepsilon_B\mu_B + ab(\varepsilon_A\mu_B + \varepsilon_B\mu_A)}{d^2}\right], \tag{17}$$

which allows us to define an effective index of refraction $n_{\text{eff}}(\omega)$ for the superlattice nanostructure given by

$$k^2 = \frac{\omega^2}{c^2}n_{\text{eff}}^2(\omega). \tag{18}$$

By assuming Drude-type responses for medium B, one obtains

$$k^2 \simeq \frac{\omega^2}{c^2}\left(\frac{a\mu_A + b\mu_0}{d}\right)\left(1 - \frac{\omega_\mu^2}{\omega^2}\right)\left(\frac{a\varepsilon_A + b\varepsilon_0}{d}\right) \times \left(1 - \frac{\omega_\varepsilon^2}{\omega^2}\right). \tag{19}$$

Using that $n_{\text{eff}}^2(\omega) = \mu_{\text{eff}}(\omega)\varepsilon_{\text{eff}}(\omega)$, it is straightforward to choose

$$\mu_{\text{eff}}(\omega) = \left(\frac{a\mu_A + b\mu_0}{d}\right)\left(1 - \frac{\omega_\mu^2}{\omega^2}\right), \tag{20}$$

$$\varepsilon_{\text{eff}}(\omega) = \left(\frac{a\varepsilon_A + b\varepsilon_0}{d}\right)\left(1 - \frac{\omega_\varepsilon^2}{\omega^2}\right), \tag{21}$$

and, therefore, the dispersion is the same that one would obtain by considering a homogeneous effective medium with Drude-type responses at shifted electric and magnetic plasmon frequencies.

By supposing, without loss of generality, that $\omega_\mu < \omega_\varepsilon$, we immediately see that $n_{\text{eff}}^2 < 0$ for $\omega_\mu < \omega < \omega_\varepsilon$, corresponding to imaginary values of k. In other words, a gap appears between ω_μ and ω_ε, as the wave can not propagate. Clearly, $n_{\text{eff}}^2 > 0$ for $\omega < \omega_\mu$ and $\omega > \omega_\varepsilon$.

For $\theta \neq 0$, it is instructive to study the limit, as $\theta \to 0$, of the three roots in Eqs. (12) and (13). In this case, the first root is given by Eq. (12) and one obtains, for Eq. (13),

$$\omega_\pm^2 \to \tfrac{1}{2}\left(\bar{\omega}_m^2 + \omega_\varepsilon^2\right) \pm \tfrac{1}{2}\left|\bar{\omega}_m^2 - \omega_\varepsilon^2\right|, \tag{22}$$

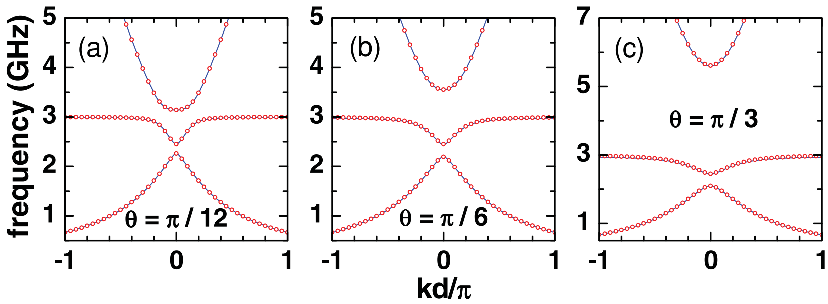

FIG. 1. (Color online) TE frequency band structure of a 1D photonic superlattice with $a = 6$ mm and $b = 12$ mm, and for $\varepsilon_0 = 1.21$, $\mu_0 = 1.0$, $\mu_A = \varepsilon_A = 1$, and $\frac{\omega_e}{2\pi} = \frac{\omega_m}{2\pi} = 3$ GHz. Solid lines were computed by solving the transcendental equation (4), whereas open circles correspond to the analytic results given by Eq. (24).

which leads to the two roots $\omega_+ \to \bar{\omega}_m$, $\omega_- \to \omega_\varepsilon$, if $\bar{\omega}_m > \omega_\varepsilon$, and $\omega_+ \to \omega_\varepsilon$, $\omega_- \to \bar{\omega}_m$, if $\bar{\omega}_m < \omega_\varepsilon$. Note that $l_0 > d$, $\omega_\mu < \bar{\omega}_m$, and $\omega_\varepsilon < \bar{\omega}_e$. Here, it should be noted that, for $\theta = 0$, the magnetic (electric) plasmon frequency $\bar{\omega}_m$ ($\bar{\omega}_e$) is not a root, and one is left with the two other roots [cf. Eqs. (15) and (16)], which define the $\langle n \rangle = 0$ gap, as we have shown.

For $\theta \neq 0$, the three roots [Eqs. (12) and (13)] give rise to *two* gaps, as we will show. In order to see this, we examine the $\theta \neq 0$ generalization of Eq. (17):

$$k^2 \simeq \frac{\omega^2}{c^2 d^2}\Big[a^2 \varepsilon_A \mu_A \cos^2\theta + b^2(\varepsilon_B \mu_B - \varepsilon_A \mu_A \sin^2\theta) + ab\left(\varepsilon_A \mu_B \cos^2\theta + \varepsilon_B \mu_A - \frac{\varepsilon_A \mu_A^2}{\mu_B}\sin^2\theta\right)\Big]. \quad (23)$$

By choosing Drude-type responses for medium B, one arrives at

$$k^2 \simeq \frac{\omega^2}{c^2}\frac{L_\theta}{d}\left(\frac{a\mu_A + b\mu_0}{d\mu_0}\right)\left(\frac{\omega^2}{\omega^2 - \bar{\omega}_m^2}\right)\left(1 - \frac{\omega_\mu^2}{\omega^2}\right) \times \left(1 - \frac{\omega_-^2}{\omega^2}\right)\left(1 - \frac{\omega_+^2}{\omega^2}\right), \quad (24)$$

and a simple analysis shows that there are two possibilities: either $\omega_\mu < \omega_- < \omega_+$ or $\omega_- < \omega_\mu < \omega_+$.

As before, we use Eq. (18) to arrive at an effective index of refraction

$$n_{\text{eff}}^2 = \frac{L_\theta}{d}\left(\frac{a\mu_A + b\mu_0}{d\mu_0}\right)\left(\frac{\omega^2}{\omega^2 - \bar{\omega}_m^2}\right)\left(1 - \frac{\omega_\mu^2}{\omega^2}\right) \times \left(1 - \frac{\omega_-^2}{\omega^2}\right)\left(1 - \frac{\omega_+^2}{\omega^2}\right). \quad (25)$$

A careful analysis of the sign of n_{eff}^2 shows that the regions where this quantity is negative correspond to the $\langle n \rangle = 0$ and to the PP gaps. These gaps, therefore, correspond to regions of the low-energy spectrum where the homogeneous effective medium is absorptive, exhibiting an imaginary effective refraction index. In fact, there are two possibilities: (i) either (ω_μ,ω_-) and ($\bar{\omega}_m$,ω_+) correspond to the $\langle n \rangle = 0$ and PP gaps, respectively; (ii) or (ω_-,ω_μ) and ($\bar{\omega}_m$,ω_+) correspond to the $\langle n \rangle = 0$ and PP gaps, respectively. For $\theta = 0$, the plasmon frequencies of the effective medium are ω_μ and ω_ε. We refer to Fig. 1, in which the TE band structure, displaying both numerical and analytical results, illustrates both the $\langle n \rangle = 0$ and PP gaps for $\theta = \frac{\pi}{12}$, $\theta = \frac{\pi}{6}$, and $\theta = \frac{\pi}{3}$. One notes that the numerical results [Eq. (4)] are in excellent agreement with the analytical ones [Eq. (24)]. In Fig. 2, both numerical [obtained via Eq. (4); represented by dark zones] and analytical [Eqs. (12) and (13); represented by dashed lines] results for the gap profiles, as a function of the incidence angle, are depicted for various values of

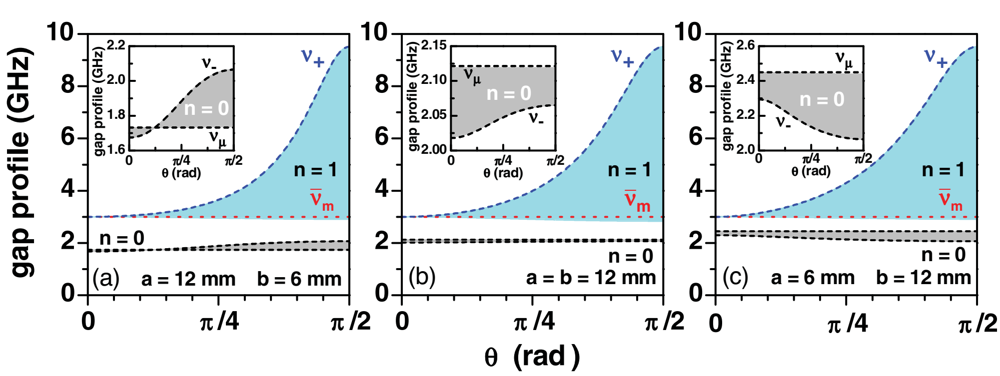

FIG. 2. (Color online) Gap profiles for TE waves, as functions of the incidence angle, associated with 1D photonic superlattices. The $\langle n \rangle = 0$ gap is labeled as $n = 0$, whereas the plasmon-polariton gap is denoted by $n = 1$. Calculations were performed for various values of the widths a and b, and for $\varepsilon_0 = 1.21$, $\mu_0 = 1.0$, $\mu_A = \varepsilon_A = 1$, and $\frac{\omega_e}{2\pi} = \frac{\omega_m}{2\pi} = 3$ GHz. In the panels, $\nu_\pm = \frac{\omega_\pm}{2\pi}$, $\nu_\mu = \frac{\omega_\mu}{2\pi}$, and $\bar{\nu}_m = \frac{\bar{\omega}_m}{2\pi}$. Dark zones correspond to numerical calculations of the gap profiles by using Eq. (4), whereas dashed lines in (a), (b), and (c) correspond to the analytic results obtained via Eqs. (12) and (13). Details of the $n = 0$ gaps are displayed in the insets.

layer widths, illustrating the agreement between analytical and numerical results.

Summing up, we have made a thorough investigation of the photonic band structure of a metastack by studying the dispersion relation, both numerically and analytically. We have calculated the null-average refractive-index gap profile as well as the PP-gap profile in a TE configuration. Of course, in the case of TM waves, one finds basically the same properties. We have chosen to present the results for the TE configuration, as PP excitations in this case have a magnetic origin, due to the enhanced magnetic component of the electromagnetic field exhibited by the metamaterial. It is worthwhile to point out that previous studies[19,20] on oblique incidence in metastacks have missed the PP gap, as they have restricted the study in the frequency region around the $\langle n \rangle = 0$ gap. We do hope that this study will be useful and inspiring for future experimental work in the area.

We thank CNPq, FAPESP, FAPERJ, and FUJB, as well as the Colombian Agency CODI (University of Antioquia) for partial financial support.

[1] R. A. Shelby, D. R. Smith, and S. Schultz, Science **292**, 77 (2001).

[2] W. L. Barnes, A. Dereux, and T. W. Ebbesen, Nature (London) **424**, 824 (2003).

[3] A. Ramakrishna, Rep. Prog. Phys. **68**, 449 (2005).

[4] E. Ozbay, Science **311**, 189 (2006).

[5] C. M. Soukoulis, S. Linden, and M. Wegener, Science **315**, 47 (2007).

[6] H. J. Lezec, J. A. Dionne, and H. A. Atwater, Science **316**, 430 (2007).

[7] J. Valentine *et al.*, Nature (London) **455**, 376 (2008).

[8] M. Dragoman and D. Dragoman, Prog. Quantum Electron. **32**, 1 (2008).

[9] S. Xiao, V. P. Drachev, A. V. Kildishev, X. Ni, U. K. Chettiar, H.-K. Yuan, and V. M. Shalaev, Nature (London) **466**, 735 (2010).

[10] J. Pacheco Jr., T. M. Grzegorczyk, B.-I. Wu, Y. Zhang, and J. A. Kong, Phys. Rev. Lett. **89**, 257401 (2002); G. V. Eleftheriades, A. K. Iyer, and P. C. Kremer, IEEE Trans. Microwave Theory Tech. **50**, 2702 (2002); A. Grbic and G. V. Eleftheriades, J. Appl. Phys. **92**, 5930 (2002); H. Jiang, H. Chen, H. Li, Y. Zhang, and S. Zhu, Appl. Phys. Lett. **83**, 5386 (2003).

[11] J. B. Pendry, Phys. Rev. Lett. **85**, 3966 (2000).

[12] U. Leonhardt, Science **312**, 1777 (2006).

[13] J. B. Pendry *et al.*, Science **312**, 1780 (2006).

[14] J. Li, L. Zhou, C. T. Chan, and P. Sheng, Phys. Rev. Lett. **90**, 083901 (2003); J. Li, D. Zhao, and Z. Liu, Phys. Lett. A **332**, 461 (2004); N. C. Panoiu, R. M. Osgood, Jr., S. Zhang, and S. R. J. Brueck, J. Opt. Soc. Am. B **23**, 506 (2006); Y. Xiang, X. Dai, and S. Wen, *ibid.* **24**, 2033 (2007); S. Kocaman, R. Chatterjee, N. C. Panoiu, J. F. McMillan, M. B. Yu, R. M. Osgood, D. L. Kwong, and C. W. Wong, Phys. Rev. Lett. **102**, 203905 (2009).

[15] S. B. Cavalcanti, M. de Dios-Leyva, E. Reyes-Gómez, and L. E. Oliveira, Phys. Rev. B **74**, 153102 (2006); Phys. Rev. E **75**, 026607 (2007); A. Bruno-Alfonso, E. Reyes-Gómez, S. B. Cavalcanti, and L. E. Oliveira, Phys. Rev. A **78**, 035801 (2008).

[16] E. Reyes-Gómez, D. Mogilevtsev, S. B. Cavalcanti, C. A. A. de Carvalho, and L. E. Oliveira, Europhys. Lett. **88**, 24002 (2009).

[17] E. Reyes-Gómez, N. Raigoza, S. B. Cavalcanti, C. A. A. de Carvalho, and L. E. Oliveira, Phys. Rev. B **81**, 153101 (2010); D. Mogilevtsev, E. Reyes-Gómez, S. B. Cavalcanti, C. A. A. de Carvalho, and L. E. Oliveira, Phys. Rev. E **81**, 047601 (2010); E. Reyes-Gómez, N. Raigoza, S. B. Cavalcanti, C. A. A. de Carvalho, and L. E. Oliveira, J. Phys. Condens. Matter **22**, 385901 (2010).

[18] D. Mogilevtsev, F. A. Pinheiro, R. R. dos Santos, S. B. Cavalcanti, and L. E. Oliveira, Phys. Rev. B **82**, 081105(R) (2010).

[19] M. Liscidini and L. C. Andreani, Phys. Rev. E **73**, 016613 (2006).

[20] H. Daninthe, S. Foteinopoulou, and C. M. Soukoulis, Photon. Nanostruct.: Fund. Appl. **4**, 123 (2006); S. K. Awasthi, A. Mishra, U. Malaviya, and S. P. Ojha, Solid State Commun. **149**, 1379 (2009).